Biophys. Struct. Mechanism 1, 239–257 (1975)

Interpretation of Invertebrate Photoreceptor Potentials in Terms of a Quantitative Model

Lorenz Kramer

Institut für Festkörperforschung der Kernforschungsanlage Jülich
and Physik-Department der Technischen Universität München

Received March 3, 1975

Abstract. It is known from voltage-clamp experiments on visual cells of *Limulus* and *Balanus* that the total membrane current can be separated approximately into a dark current J_D and a light-induced current J_L such that each part has a time- and intensity-independent reversal potential. In addition J_L can be represented approximately as a product of a non-linear, time-independent current-voltage characteristics $J^0{}_L(V)$ and an "activation factor" x_A

List of the more Important Symbols

A	Adaptation factor
C	ratio between slopes of current-voltage curves for maximum light-induced current and dark current
d	one half the thickness of the membrane
F_i	"effective membrane permeability", cf. Eq. (7)
g_i	electrochemical potential inside membrane
$g_i^{\leqq}$	electrochemical potential inside and outside cell
I	light intensity (quanta/sec cm²)
i	(index) refers to i-th ionic species
J	total current leaving cell
J_D	dark current
J_L	light-induced current
j_i	ionic current density inside membrane in x-direction
K	cf. Eq. (21)
k	Boltzmann's constant
k_0	rate constant for chain reaction (production of X)
k_1	rate constant for decay of X_1
k_2	rate constant for decay of X (closing of sites)
M	total number of sites controlling light conductance
N	multiplication factor in dark adapted state (maximum of Z)
n_i	density of ions inside membrane
$n_i^{\leqq}$	density of ions inside and outside cell
$p_1, p_2,$	rate constants for adaptation kinetics
p_3	cf. Eq. (29)
q	elementary charge
q_i	ionic charges
$\mathbf{r}$	$= (x, y, z)$ spatial variable
T	temperature
t	time
u	cf. Eq. (28)
V	membrane potential
V_D	reversal potential for the dark current
V_L	reversal potential for the light current
V_i	diffusion potential, cf. Eq. (8)
$V^{\leqq}$	potential steps at the inner and outer membrane surface
V_0	$= V^< - V^>$
X	$= x_A M$, number of open sites
X_1	$= x_1 M$ number of molecules of agent whose decay initiates chain reactions
x_A	degree of activation of light sensitive membrane
Y	number of sites opened by individual chain reaction
Z	multiplication factor (number of sites opened by one photoisomerized rhodopsin molecule)
ε_i	activation energy inside membrane (measured with respect to surrounding solution)
ψ	electrostatic potential
ϱ_0	fixed-charge distribution inside membrane
σ	cross section for photoisomerization of one rhodopsin molecule by a photon
$\bar{\sigma}$	$= k_1 \sigma / k_2$

which depends on light intensity and time. $J^0_L(V)$ can be described by a simple electrodiffusion membrane model (for J_D we use the same model). A set of kinetic equations including amplification, latency and light adaptation leads to a determination of x_A for photoisomerization of single rhodospin molecules and for arbitrary light signals. The receptor potentials calculated show many features of the experiments on *Limulus*, *Balanus* and *Astacus*.

Key words: Photoreceptor Model — Receptor Potential — Invertebrate.

1. Introduction

Over the past 20 years a considerable amount of electrophysiological data of the (late) photoelectric response ("receptor potential") in visual cells has been accumulated, especially for invertebrates. More recently, voltage-clamp studies have given additional insight into the electric characteristics of some photoreceptors in darkness and under illumination (for a summary, see Fuortes and O'Bryan, 1972). Whereas this activity has led to many qualitative conclusions, few authors have analysed the receptor potential in terms of quantitative models. The problem seems to be that the only simple and straightforward tool available for the analysis of complex time dependent processes, namely the expansion in a number of discrete linear first-order processes does not lead very far in the present case. The reason is that the linear response range is usually very small for photoreceptors and often experimentally not readily accessible.

Nevertheless linear response analysis has its value, especially since not only the response to small light intensities is linear, but at arbitrary intensity also the initial phase of the receptor potential, where the response is still very small. Fuortes and Hodgkin (1964), who realized this fact, proposed a (descriptive) model based on a chain of n (~ 5 to 10) linear processes which may be interpreted as electric low-pass filters including an amplifying element. The model, which has the merit of being very simple, produces an acceptable linear response for some *Limulus* data[1], describes well the latency behaviour at arbitrary intensity, and allows to correlate changes in sensitivity with changes in time scale as found in different states of adaptation. The authors also give a nonlinear extention of their model by introducing a feedback control. Their Ansatz has the important feature of coupling a decrease in sensitivity [defined as being inversely proportional to the energy of a short light stimulus necessary to evoke a response of prescribed (small) height] with an increase in time resolution as observed experimentally. The model suffers from quantitative defects and does not allow an interpretation of the voltage-clamp results published later.

Subsequently the equations of Fuortes and Hodgkin were interpreted in various ways (Borsellino *et al.*, 1965; Levinson, 1966) and, more importantly, an analysis of the stochastic properties of the response was carried out in terms of an analoguous compartmental model by Borsellino and Fuortes (1968a, b). The authors conclude that, in order to explain the observed variability of the single-photon response, the model must incorporate gain, i.e. photoisomerization of one rhodopsin molecule must influence many controlling sites.

Recently, a detailed quantitative model for the (nonlinear) response of the squid photoreceptor was proposed (Allyn and Budrikis, 1974). The model consists

[1] In our experience the fit to measurements on *Balanus* and *Astacus* and in many cases even to *Limulus* is not satisfactory.

of a somewhat complicated set of kinetic equations which determine the behaviour of the sodium permeability for any given light stimulus. The membrane potential is assumed to be at all times a diffusion potential arising from the combined action of Sodium, Potassium and Chloride. No attempt is made to explain voltage-clamp results. Whereas a number of slow processes are included, the latency behaviour of the visual response is not taken into account.

Also, a fairly specific descriptive model for the reconstruction of the electrical response of turtle cones has been published recently (Baylor *et al.*, 1974). The model is based mainly on a linear chain of rate equations determining the concentration of an agent which controls the conductivity in one of several parallel channels. Under voltage-clamp conditions the (model-) current response to a long light flash does not display a transient. Therefore the model should not be applied to invertebrates.

We here wish to propose a quantitative model which describes all features of the normal invertebrate receptor potential consistent with voltage-clamp results. In designing this model our aim was not just to obtain quantitative agreement with experiments but to provide a framework from which to proceed toward an understanding of the underlying mechanisms. Thus we hope that, although at present definite mechanisms can scarcely be offered and the specific form of the equations is often chosen by convenience rather than dictated by necessity, the basic elements and the structure of the model reflect in some way the functional organization of a photoreceptor. As it stands the model is certainly not in its final form but will need continuous improvement, without, hopefully, changing the basic concepts.

Our starting point is the voltage-clamp investigation on *Limulus* (Milecchia and Mauro, 1969b) and *Balanus* (Mack Brown *et al.*, 1970; 1971). There the dark current J_D is observed to have an approximately time-independent reversal potential V_D and similarly the light-induced current possesses a time- as well as (light) intensity-independent reversal potential V_L. This holds true for the time scale of the normal receptor potential, i.e., as long as one neglects very rapid transients (probably due to capacitive discharge) and very slow changes (Lisman and Brown, 1971). Thus we write (symbolically)

$$J = J_D\,(V - V_D, t) + J_L\,(V - V_L, \mathrm{I}, t), \tag{1}$$

where J_D and J_L are zero for all times t and light intensities I if their first argument is zero (V = voltage across the membrane). Moreover it is found that the light current can approximately be written in the form

$$J_L\,(V - V_L, I, t) = x_A\,(I, t)\,J_L^0\,(V), \tag{2}$$

where $J_L{}^0$ is time- and intensity-independent and the quantity x_A does not depend on voltage[2] (in the dark $x_A = 0$).

The simplest interpretation of Eqs. (1) and (2) is in terms of two kinds of regions (or channels) in the membrane which have different ionic selectivities and therefore different diffusion potentials V_D and V_L. The light sensitive region can be in a "closed" or "open" state, and the size of the open region (or number of open channels) is proportional to the "activation factor" x_A.

[2] Deviations from Eq. (2) appear to exist for *Balanus* within about 40 ms after a sudden change of voltage (Mack Brown, 1970).

It is a straightforward task to understand the rectifying current-voltage characteristics $J_L^0(V)$ in terms of well-known fixed charge membrane concepts (see e.g. Teorell, 1953; Coster, 1965). In Sect. 2 we present a version of this model where the density of mobile ions inside the membrane is assumed small, i.e. the activation energy for penetration into the membrane is sufficiently large. Some attention is given to the example where the fixed charges simply consist of dipole layers near the membrane surfaces. The model demonstrates how changes in conductance can result from changes in the fixed-charge distribution which in turn could couple to some photochemical process.

Unfortunately no equally good description of the dark current can at present be offered, since both, the time- and voltage-dependence of J_D are more complicated. For simplicity we adopt the same (time-independent) current-voltage curve as for J_L^0, except replacing V_L by V_D. The relation $J=0$, which represents the continuity equation (displacement currents are neglected) then leads to a simple expression for the receptor potential of the free (i.e. not clamped) cell as a function of x_A. The expression exhibits a logarithmic response range for intermediate activations (Weber-Fechner Law).

Sect. 3 contains a kinetic model determining x_A for any light stimulus. The total response is treated as a superposition of elementary responses, each resulting from photoisomerization of one rhodopsin molecule. The necessary amplification and latency of the elementary response comes mainly from a process which is most simply interpreted in terms of a saturating chain-reaction. Light-induced desensitization is brought in by having the total "output" x_A control the saturation point of the chain reactions. In this way a decrease in sensitivity (light adaptation) is coupled to an increase in time resolution. Plots of the model-response for various choices of parameters and light signals are shown and compared with experiments on *Limulus*, *Balanus* and *Astacus*. After turning off a light stimulus, but maintaining a background illumination, the response curve displays a transient hyperpolarization. The changes in the receptor potential observed experimentally when the concentration of Ca is reduced in the outside medium can be simulated quantitatively by reducing the effect of light adaptation. In Sect. 4 some special features, deficiencies and possible improvements of the model are discussed.

2. The Electrodiffusion Model

Let the plane of the membrane coincide with the y-z plane of a coordinate system and let the inner and outer surfaces of the membrane be given by $x=-d$ and $x=+d$, respectively. The passive currents are driven by the gradients of the electrochemical potentials g_i for the different ionic species. For small gradients one has at point $\mathbf{r}$ inside the membrane

$$j_i(\mathbf{r}) = -q_i \mu_i(\mathbf{r}) n_i(\mathbf{r}) \frac{dg_i(\mathbf{r})}{dx}. \tag{3}$$

Here j_i is the current density in the x direction, q_i the ionic charge, μ_i the mobility and n_i the density for the i-th ionic species (we use molecular and not molar units). For low density of mobile ions inside the membrane one may make the Ansatz

$$g_i = kT \ln n_i + \varepsilon_i(\mathbf{r}) + q_i \psi(\mathbf{r}) \tag{4}$$

where k is Bolzmann's constant, T the temperature, ε_i the activation energy ($\varepsilon_i = 0$ outside the membrane) and ψ the electrostatic potential. Making the assumption that the mobilities μ_i are small compared to those in the solution on either side we may set the electrochemical potential outside the membrane equal to constants given by

$$g_i^< = kT \ln n_i^< + q_i^< \; V \text{ for } x < -d \; ;$$
$$g_i^> = kT \ln n_i^> \qquad \text{for } x > d \; . \tag{5}$$

Here $n_i^<$ and $n_i^>$ are the ionic densities inside and outside the cell. The same assumption allows one to neglect currents flowing inside the membrane in the y- and z-direction so that in the stationary state j_i does not depend on x.

Eq. (3) together with (4) is now an ordinary linear first-order differential equation which can be solved. Imposing the conditions that g_i is continuous at $x = \pm d$ one obtains for the current

$$j_i(y, z) = q_i \, kT \, F_i(y, z) \, n_i^< \, (e^{q_i(V - V_i)/kT} - 1) \; , \tag{6}$$

where

$$F_i(y, z) = [\int_{-d}^{d} dx \, \mu_i^{-1}(\mathbf{r}) \exp(\varepsilon_i(\mathbf{r}) + q_i \psi(\mathbf{r}))/kT]^{-1} \; , \tag{7}$$

$$V_i = \frac{kT}{q_i} \ln \frac{n_i^>}{n_i^<} \; . \tag{8}$$

The quantity F_i represents a kind of effective membrane permeability. Note that ψ (and therefore also F_i) still depends on V. This dependence can in principle be made explicit for a given distribution of fixed charges ϱ_0 by solving Poisson's equation inside and outside the membrane. Calculations become especially simple if one assumes that the electrolyte-membrane-electrolyte system acts, as far as the charge distribution is concerned, like an ordinary condenser, i.e. a change in voltage V produces only additional surface charges of opposite sign at $x = \pm d$. Then one finds

$$\psi(x) = \psi_0(x) - V \frac{x - d}{2d} \; , \tag{9}$$

where ψ_0 is the potential distribution for $V = 0$. This approximation is good as long as the Debye length λ_D is large compared to $2d$ inside the membrane and small compared to $2d$ in the electrolytes[3]. Eqs. (6) to (9) determine the current-voltage characteristics of the membrane. One easily sees that $F_i(V)$ is a monotonically decreasing function whereas $j_i(V)$ increases monotonically. Notice that highly nonlinear current voltage characteristics can be produced in spite of the linear relation between current and driving force (3). This is of course connected with the fact that inside the membrane n_i depends critically on ψ, which in turn depends on V.

A particularly simple and possibly sometimes quite realistic example is that of a membrane which is homogeneous and neutral in its interior ($\varepsilon_i = \text{const.}$, $\mu_i = \text{const.}$, $\varrho_0 = 0$) except for the existence of dipole layers at $x = \pm d$. Then one has

$$\psi_0(x) = V^< \frac{x - d}{2d} - V^> \frac{x + d}{2d} \tag{10}$$

[3] For univalent ions one has $\lambda_D = (\varepsilon \, kT/nq^2)$, where ε is the dielectric constant and n the total density of mobile ions. For a millimolar solution of (positive and negative) ions in water λ_D is about 1.5 nm.

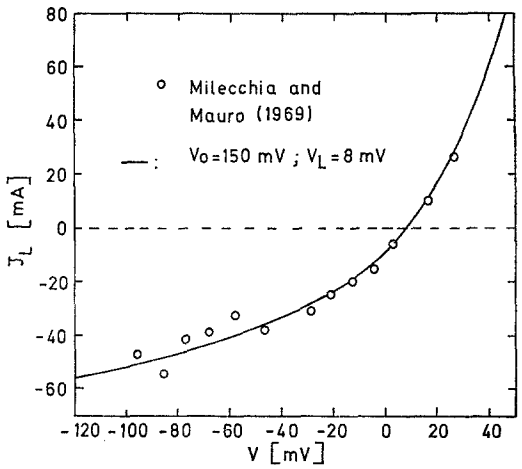

Fig. 1. Current-voltage relation as given by Eq. (11) and voltage-clamp results for the peak current induced by a step-like light signal in the ventral eye of *Limulus* (Milecchia and Mauro, 1969b, Fig. 4b)

where $V^<$ and $V^>$ are the potential steps produced by the membrane-bound dipol layers and the adjacent electrolyte at $x = -d$ and $x = +d$, respectively. From Eqs. (6), (7), (9) and (10) one obtains

$$j_i = c_i \frac{q_i (V - V_0)/kT}{e^{q_i (V-V_0)/kT} - 1} (e^{q_i (V-V_i)/kT} - 1), \tag{11}$$

where

$$c_i = \mu_i \exp(-\varepsilon_i + q_i V^>)/kT. \tag{12}$$

Here $V_0 = V^< - V^>$ denotes the asymmetry of the potential steps.

In Fig. 1 the relation (11) has been plotted for $V_0 = 150$ mV, $V_i = 8$ mV and $T = 20°$ C taking for q_i the elementary charge q. Voltage-clamp measurements of the peak light current induced by a step-like signal in the ventral eye of *Limulus* (Milecchia and Mauro, 1969b) have been included. Using the same parameters and merely changing a forfactor (which was adjusted in Fig. 1 to give a good fit) one can describe the results for the light current in the stationary state and the current-voltage characteristics for the slow potential fluctuations. Of course the shape of the curve remains unchanged if several univalent ions contribute to the current. One then has to replace V_i by the combined diffusion potential V_R which is for this simple model

$$V_R = \frac{kT}{q} \ln \frac{\sum_i c_i}{\sum_i c_i \exp(-q V_i/kT)}. \tag{13}$$

Eqs. (11) and (12) also demonstrate how the conductance is effected by changes in the charge distribution. When $V^<$ and $V^>$ are increased by 150 mV the current is reduced by a factor 400. For the parameters used in Fig. 1 a comparable effect is obtained in the relevant voltage range if $V^<$ alone is reduced by 150 mV or if $V^>$ is increased by 300 mV. Such a change thus essentially "closes" the effected region of the membrane.

Now returning to the general case we represent the light-induced current by an expression of the type

$$J_L = x_A F(V) (e^{q(V-V_L)/kT} - 1), \tag{14}$$

where $F(V)$ is, up to a constant factor, a function of the type given in Eq. (7). In Eq. (14) we have integrated the current density over the light-sensitive part of the membrane and summed over all mobile ions, which are assumed to be univalent. The activation factor x_A which is proportional to the size of the "open" membrane area (or number of "open" channels) depends on light stimulus but not on voltage. We choose the maximum value of x_A to be 1.

Unfortunately, the dark current J_D cannot be represented with comparable accuracy by this simple electrodiffusion model because one would have to assume a *voltage*-dependent structural change in the membrane (e.g. like the activation above) in order to explain the time dependence and the quantitative shape of the current-voltage curve. Before constructing a proper model more and better experimental data are needed. For simplicity we here use for J_D the same expression as for J_L except that V_L is replaced by the dark potential V_D and x_A is replaced by a constant:

$$J_D = C^{-1} F(V) \left(e^{q(V-V_D)/kT} - 1\right). \tag{15}$$

Comparing the observed dark current with the maximum light current one finds $C \approx 20$ to 40 for *Limulus* (Milecchia and Mauro, 1969b) whereas for *Balanus* C is probably larger (Mack Brown *et al.*, 1970; 1971). Now setting the total current equal to zero[4] one obtains

$$V - V_D = \frac{kT}{q} \ln \frac{1 + C\,x_A}{1 + \alpha C\,x_A}\,; \tag{16}$$

$$\alpha = \exp\left[-q(V_L - V_D)/kT\right]. \tag{17}$$

For *Limulus* $V_L - V_D$ is about 60 mV so that $\alpha \sim 0.1$, whereas for *Balanus* α is somewhat smaller.

According to Eq. (16) the depolarization depends on x_A linearly for $Cx_A \ll 1$ and the dependence becomes approximately logarithmic in the region $Cx_A \gg 1$, $\alpha C x_A \ll 1$. If $\alpha C \gg 1$ holds the potential approaches its saturation value V_L before x_A saturates. From Eqs. (14) and (15) one can also calculate the differential resistance of the membrane. One finds that it decreases monotonically with increasing depolarisation as found experimentally (Stieve, 1965). There does not, however, exist a range where the resistance depends logarithmically on x_A.

3. Activation Kinetics and Results

We here propose a set of kinetic equations to describe the main features of the activation of the light sensitive membrane. This part of the model is rather speculative and instead of attaching too much significance to the specific form of some of the equations we wish to emphasize their general structure.

a) Response to Single Photons and to Weak Light

Our starting point is the assumption that the slow potential fluctuations ("bumps") observed in some photoreceptors at low light intensity are connected with photoisomerization of single rhodopsin molecules. From the observed large size which bumps can acquire one concludes that the area of the membrane activated cannot be of molecular dimension (see Cone, 1973). There must exist an

[4] The total active transport current is assumed to be zero.

amplification mechanism which spreads out the activation over some large fraction of the light-sensitive membrane. We treat the kinetics of this process as a chain reaction with some kind of saturation, although other interpretations making use of cooperative interactions seem possible. At present there is no evidence for the existence of a direct cooperative interaction between rhodopsin molecules, and we therefore prefer to think of the interaction mechanism necessary to provide the amplification as an *irreversible* energy transfer. Determination of this mechanism remains of central importance.

We visualize the light-induced conductance as being controlled by a large number of sites, and there may in fact exist a one-to-one correspondence between these sites and the rhodopsin molecules (M = number of sites $\sim 10^8$ to 10^{10}). Photoisomerization of a rhodopsin leads to the opening of one site and this sets off a chain reaction. Subsequent activations take place without isomerization of rhodopsin. The initial-value problem

$$\dot{Y} = k_0 Y(1 - Y/Z) \; ; \qquad Y(t_0) = 1 \tag{18}$$

(Y = number of sites activated) describes such a process where the first site is opened at time $t = t_0$. Here saturation is introduced in the simplest possible manner and Z ($1 \ll Z \ll M$) is the total number of sites opened by one isomerized rhodopsin ("multiplication factor")[5]. Note that the differential Eq. (18) has one stable ($Y \equiv Z$) and one unstable ($Y \equiv 0$) stationary solution. Therefore one could interpret the closed state of the light-sensitive membrane as a metastable configuration of the system. Photoisomerization of a rhodopsin provides the energy to overcome the barrier so that a fraction of the membrane can "fall" into the open state.

The solution of Eq. (18) is given by

$$Y(t, t_0) = \theta(t - t_0) \frac{Z\, e^{k_0(t-t_0)}}{Z - 1 + e^{k_0(t-t_0)}} \approx \theta(t - t_0) \frac{e^{k_0(t-t_0)}}{1 + e^{k_0(t-t_0)}/Z} \tag{19}$$

($\theta(x) = 0$ for $x < 0$ and $= 1$ for $x > 0$). Assuming first-order kinetics for the backward reaction the number of open sites X is determined by the equation

$$\dot{X} = -k_2 X + K(t, t_0) \; , \tag{20}$$

where

$$K(t, t_0) \; [= dY(t, t_0)/dt_0] = -dY(t, t_0)/dt_0 \; . \tag{21}$$

In Fig. 2 we have plotted $X(t - t_0)$ (normalized to its value at the maximum) for $Z = 10^5$, $k_0 = 100\ \mathrm{sec}^{-1}$ and various values of k_2. For $k_2 \gg k_0$ one simply has $X = K(t, t_0)/k_2$ and for $k_2 \ll k_0$ the relation $X = Y(t, t_0) \exp[k_0 (t - t_0)]$ holds. Since the degree of activation $x_A \equiv X/M$ is small for a single-photon response, the depolarization $V - V_D$ is proportional to X. From the average shape of the slow potential fluctuations in *Limulus* (Stieve, 1965, Fig. 9; Milecchia and Mauro, 1969a, Fig. 5) one estimates $k_2 \sim 20\ \mathrm{sec}^{-1}$.

The curves in Fig. 2 display a latency behaviour which forms the basis for the latency of the full response. Whereas the response follows the stimulus with a

[5] One might be tempted to interpret Eq. (18) in terms of an ordinary second-order autocatalytic reaction. One would then have to take k_0 proportional to Z. Since light adaptation will be simulated by letting Z vary and keeping k_0 fixed (see below) we do not adopt this interpretation.

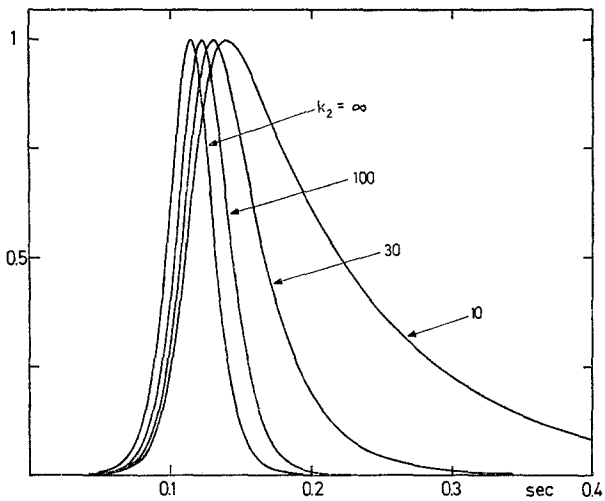

Fig. 2. Normalized response to single photoisomerization of rhodopsin for $Z = 10^5$, $k_0 = 100\ \mathrm{sec}^{-1}$ and various values of k_2

time-delay of order $k_0^{-1} \ln Z$ (the whole normalized response is simply shifted in time by changing Z, as long as $Z \gg 1$ holds) the amplitude of the response is proportional to Z. This interesting property is of importance in the context of adaptation.

We assume a chain reaction to be initiated by the decay of some photoproduct of rhodopsin whose average number of molecules X_1 is to a sufficient approximation controlled by the rate equation

$$\dot{X}_1 = -k_1 X_1 + (M - X_1)\,\sigma I\ . \tag{22}$$

Here I is the light intensity and σ the cross section for photoisomerization of one rhodopsin molecule. In reality one expects a complex sequence of events to take place between absorption of a photon and the beginning of the chain reation. Eq. (22) is supposed to describe only the rate-determining step. To obtain the total number of open sites averaged over many photon events one has to multiply $K(t, t_0)$ in Eq. (20) by the rate $k_1 X_1(t_0)$ at which chain reactions are initiated and integrate over time. Thus one is left with

$$\dot{X} = -k_2 X + k_1 \int_{-\infty}^{t} dt'\, K(t, t')\, X_1(t')\ . \tag{23}$$

It is convenient to define normalized quantities $x_1 = X_1/M$ and $x_A = X/M$ and to introduce an auxiliary variable x_2 by the equation

$$x_A = k_2 (x_2 - x_A)\,. \tag{24}$$

Assuming $x_1 \ll 1$ one obtains from (22) to (24)

$$\dot{x}_2 = -k_1 x_2 + \bar{\sigma} \int_{-\infty}^{t} dt'\, K(t, t')\, I(t')\ , \tag{25}$$

where

$$\bar{\sigma} = k_1 \sigma / k_2\ . \tag{26}$$

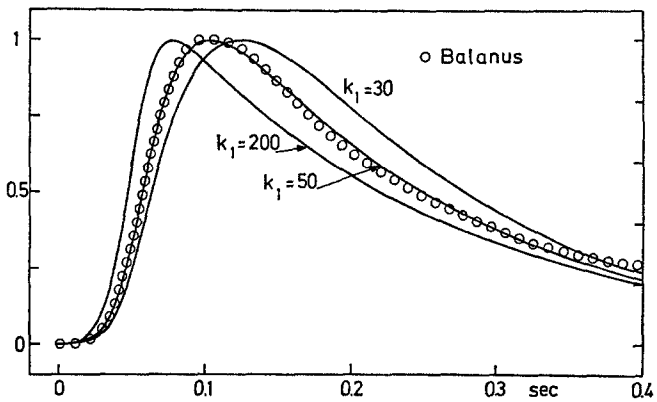

Fig. 3. Normalized response to a short, weak light flash for $Z = 250$, $k_0 = 120$ sec^{-1}, $k_2 = 5$ sec^{-1} and various values of k_1. Included is a extracellularly recorded receptor potential from the lateral eye of *Balanus* (Krischer, 1970, Fig. 1), $T = 13°$ C, relative intensity = 0.3

The reason we have derived Eqs. (24), (25) is that in this form the problem is easier to handle computationally. Eqs. (24), (25) suggest, however, a direct reinterpretation which would lead to differences in the single-photon response and the response to strong light.

In Fig. 3 the response x_A (normalized to its value at the maximum) to a very short light flash is plotted for $Z = 250$, $k_0 = 120$ sec^{-1}, $k_2 = 5$ sec^{-1} and various values of k_1. Also included is a receptor potential from the lateral eye of *Balanus* measured extracellulary in the linear range (one expects the extracellular signal to be proportional to the intracellular one at least in the linear regime). The curve with $k_1 = 50$ sec^{-1} exhibits the best fit.

Here we must point out a peculiarity of the model: One easily sees from Eqs. (24) and (25) that interchanging k_1 and k_2 changes the response only by a multiplicative factor and therefore leaves the model-response in Fig. 3 unaltered. The two cases do, however, differ in the nonlinear range and the choice taken in Fig. 3 is probably correct for *Balanus*.

Similar good fits can be achieved for other animals, and for the lateral eye of *Limulus* one finds $k_0 \sim 100$ sec^{-1}, $k_1 \sim 10$ sec^{-1}, $k_2 \sim 20$ sec^{-1} (some measurements are shown in Fig. 7). For highly dark adapted eyes of *Limulus* one has to take $Z \sim 10^6$ whereas Z is smaller in a light adapted state.

In the linear range the response to an arbitrary stimulus is always obtained as a superposition of responses to a (continuous) sequence of short stimuli. It follows that no transient (maximum) occurs in the response to a long weak step of light and after turning off such a stimulus the response persists for a time ("persistence time") equal to the latency time at the beginning.

b) Response to Strong Light

Up to this point different chain reactions were treated as independent and the model includes nonlinearities only through the nonlinear current-voltage relation of the membrane [i.e. Eq. (16)] and the saturation in Eq. (22). As a result of the multiplication one has $x_A \gg x_1$. Therefore nonlinearities connected with x_A

becoming large are expected to be of importance for intensities, where x_1 is still small, and we will continue to neglect the saturation in Eq. (22). The nonlinearities describing the effect of light adaptation will be incorporated (and this is one of the essential points of the model) in an approximate manner by letting the multiplication factor Z vary in time and in fact depend functionally on x_A. In this way one can understand the following phenomena which are otherwise difficult to explain:

1. The reduced size of the bumps in a less sensitive (light adapted) state.
2. The shortened time-delay of the response in a less sensitive state of adaptation.
3. The shortening of the persistence time with increasing intensity [see Fig. 6; the shortening of the latency time is a much more trivial effect (see Sect. 4)].

Thus we let Z in Eq. (19) depend on t and write

$$Z(t) = N\,[1 - x_A(t)]\,A(t)\,. \tag{27}$$

Here N is the multiplication factor in the most dark adapted state, the factor $1 - x_A$ expresses an instantaneous restriction for the chain reactions averaged over the whole cell, and $A(t)$ incorporates time-delayed "membrane" adaptation. We found it convenient to write

$$A(t) = \mathrm{e}^{-u(t)} \tag{28}$$

and we used the following kinetic equation for u

$$\dot{u} = -\,p_1\,u + p_2\,x_A/(1 + p_3\,x_A)\,. \tag{29}$$

If one interprets Eq. (29) in terms of a chemical reaction one would understand the nonlinear Michaelis-Menthen forward rate as usual by catalytic action. It turns out that one must choose p_1 of order 1 sec^{-1} to obtain the shape of the response curves. Thus Eq. (29) does not cover slow dark adaptation effects which have time constants of order 20 sec and longer. One can, however, include such phenomena by, e.g., also having a nonlinear backward rate so that a slow component in the decay of u results. For simplicity we shall here omit such complications. Instead the value of N can be adjusted to the varying degree of long-time adaptation where necessary.

The transformation which previously led to Eq. (25) is now no longer possible. However, one still obtains from (22) and (23) the approximate equation

$$\dot{x}_2 = -\left(k_1 + \frac{\dot{x}_A}{1 - x_A} + \dot{u}\right) x_2 + \bar{\sigma} \int_{-\infty}^{t} dt'\,K(t, t')\,I(t') \tag{30}$$

which becomes rigorous for $k_0 \gg k_1$ and is again considerably easier to handle computationally. In addition to Eqs. (16), (27) to (30) the complete model now consists of

$$\dot{x}_A = k_2\,(x_2 - x_A) \tag{31}$$

$$K(t, t') = -\frac{d}{dt'}\,\theta\,(t - t')\,\frac{e^{k_0(t-t')}}{1 + e^{k_0(t-t')}/Z\,(t)}\,. \tag{32}$$

In Fig. 4a the response to a light stimulus of 1 sec duration is plotted for $k_1 = 15\ \mathrm{sec}^{-1}$, $k_2 = 150\ \mathrm{sec}^{-1}$ (for the other parameters see figure caption) and various intensities. In Fig. 4b the values for k_1 and k_2 are interchanged. Although

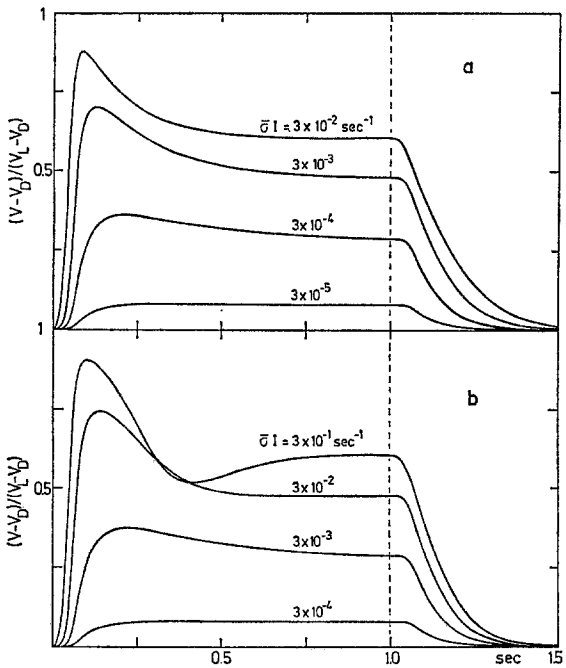

Fig. 4. a) Response to light stimulus of 1 sec duration for $N = 10^3$, $k_0 = 120$ sec^{-1}, $k_1 = 15$ sec^{-1}, $k_2 = 150$ sec^{-1}, $p_1 = 1.6$ sec^{-1}, $p_2 = 120$ sec^{-1}, $p_3 = 0$, $C = 150$, $V_L - V_D = 75$ mV and various intensities. b) The values for k_1 and k_2 are interchanged

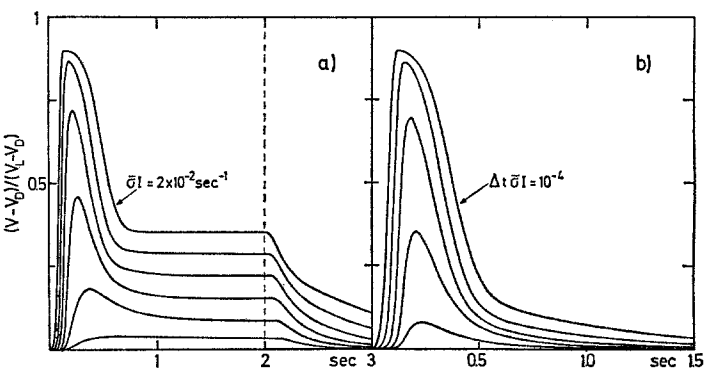

Fig. 5. Response for $N = 10^5$, $k_0 = 80$ sec^{-1}, $k_1 = 5$ sec^{-1}, $k_2 = 20$ sec^{-1}, $p_1 = 1$ sec^{-1}, $p_2 = 300$ sec^{-1}, $p_3 = 10$, $C = 40$, $V_L - V_D = 62.5$ mV. Successive curves differ by a factor of 10 in intensity. a) Light stimulus of 2 sec duration. b) Short light flash of duration Δt

the two cases exhibit an identical response for weak light (see above) characteristic differences develop at higher intensities, most notably the minimum following the transient in case b. This oszillatory behaviour does not occur for $k_2 \gg k_1$ [in this case one has $x_A \approx x_2$ so that Eq. (30) can be simplified] or too large values of p_3/p_2. Much stronger (damped) oszillations than those in Fig. 4b can be produced by

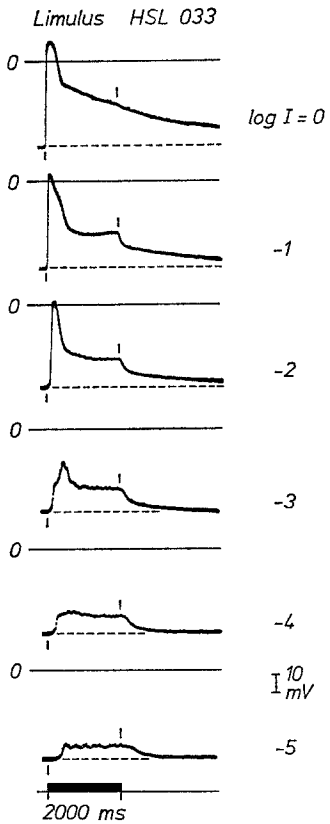

Fig. 6. Intracellular receptor potentials following light stimulus of 2 sec duration for lateral eye of *Limulus* (Stieve *et al.*, 1975) $T \approx 22°$ C, intensity in relative units

decreasing k_1 or increasing p_2 and p_3. In the lateral eye of *Balanus* one seems to observe the minimum quite systematically, and the intensity series in Fig. 4b in fact reproduces the features found, e.g., in the intracellular measurements of Mack Brown *et al.* (1970, Fig. 2; 1971, Fig. 1).

In Fig. 5 the model-response to long and short stimuli is shown for a different set of parameters. Successive curves differ by a factor of 10 in intensity. These results may be compared with intracellular measurements on the lateral eye of *Limulus* some of which are shown in Figs. 6 and 7. Whereas again the main features are reproduced quite well (except at the very highest intensities) the following quantitative disagreement exists:

1. The hight of the model-response for long stimuli at low intensity is too small. This is probably not a serious deficiency of the model but has to do with the fairly high spontaneous bump rate present in the dark in these measurements obtained at $T \approx 22°$ C. At $T = 15°$ C the discrepancy seems to disappear (Stieve, 1975).

2. The shortening of the persistence time with increasing intensity (long stimulus) seems more pronounced in the experiments than in the model.

3. After turning off a high intensity stimulus (long or short) the response exhibits a rapid and a slow decay range. In the model the slowing down of the

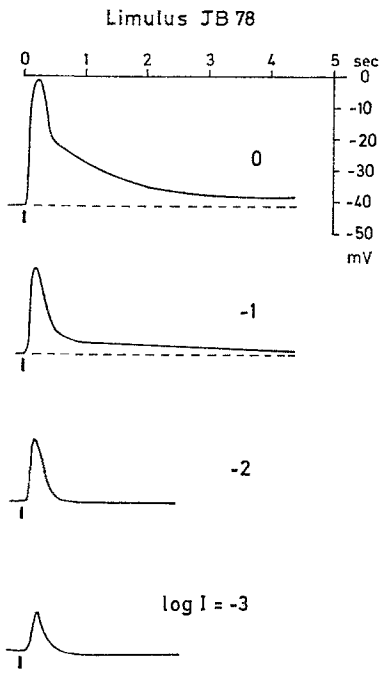

Fig. 7. Intracellular receptor potentials following light stimulus of 0.05 sec duration for lateral eye of *Limulus* (Stieve, 1974b), $T = 15°$ C, intensity in relative units

decay comes as a result of dark adaptation, i.e. the increase of A (decrease of u) setting in after x_A has started to decay. The effect becomes appreciable only when k_2 is larger than k_1. We were not, however, able to make the effect as pronounced as in the *Limulus* experiments. There is some evidence that this feature is not, or only in part, connected with a conductance change of the membrane (Stieve, 1965).

4. At very high intensities the *Limulus* response develops features which are not described by the model. It seems that a different kind of rate limitation now becomes effective.

5. In addition there exist discrepancies which come from the fact that no perfect fit has been attempted (especially for the short stimulus). One would have to choose two somewhat different sets of parameters in order to fit the response of the two different animals and temperatures used in Figs. 6 and 7.

In Fig. 8 the depolarization at the peak of the transient and in the steady state are plotted from Fig. 5a as a function of the logarithm of intensity. For the transient one obtains the well-known sigmoid curve whereas no saturation occurs (at these intensities) for the steady-state depolarisation. This is in agreement with experiments (Stieve, 1974a, Fig. 11; Milecchia and Mauro, 1969a, Fig. 3). Note that the corresponding curves taken from Fig. 4 would be steeper.

Fig. 9 demonstrates the fact that by a moderate change of parameters a model-response can be generated which is rather reminiscent of results obtained from the *Limulus* ventral eye (Milecchia and Mauro, 1969a, Fig. 1). The transient can be made sharper and the plateau lower by increasing p_2.

Figs. 10 and 11 show responses for long stimuli superimposed on a steady background light of intensity I_0. The same parameters as in Figs. 4b and 5 were

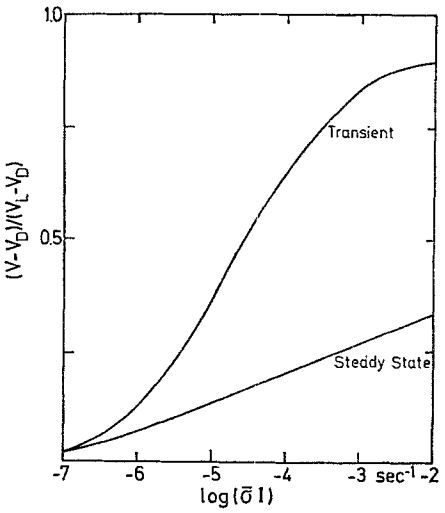

Fig. 8

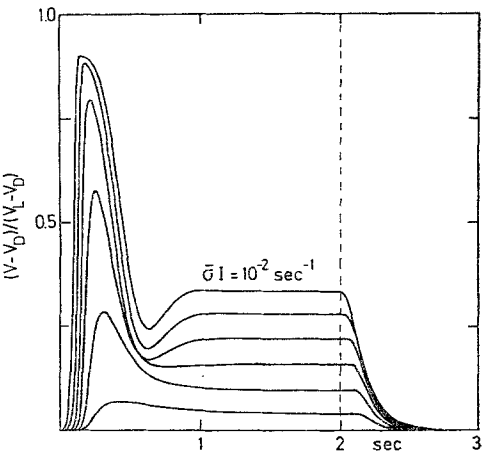

Fig. 9

Fig. 8. Depolarization at peak of transient and in the steady state as a function of logarithm of intensity. Same parameters as in Fig. 5

Fig. 9. Response to light stimulus of 2 sec duration for $N = 10^6$, $k_0 = 80\ \text{sec}^{-1}$, $k_1 = 15\ \text{sec}^{-1}$, $k_2 = 15\ \text{sec}^{-1}$, $p_1 = 1\ \text{sec}^{-1}$, $p_2 = 300\ \text{sec}^{-1}$, $p_3 = 6$, $C = 40$, $V_L - V_D = 62.5$ mV. Successive curves differ by a factor of 10 in intensity

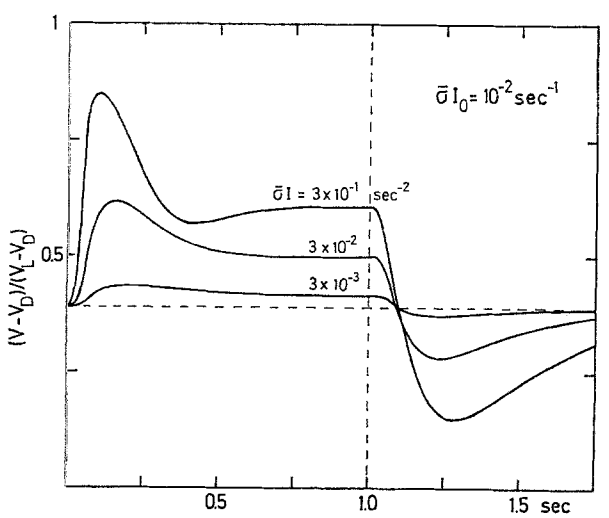

Fig. 10. Response to long stimulus superimposed on steady background light of intensity I_0. Same parameters as in Fig. 4b

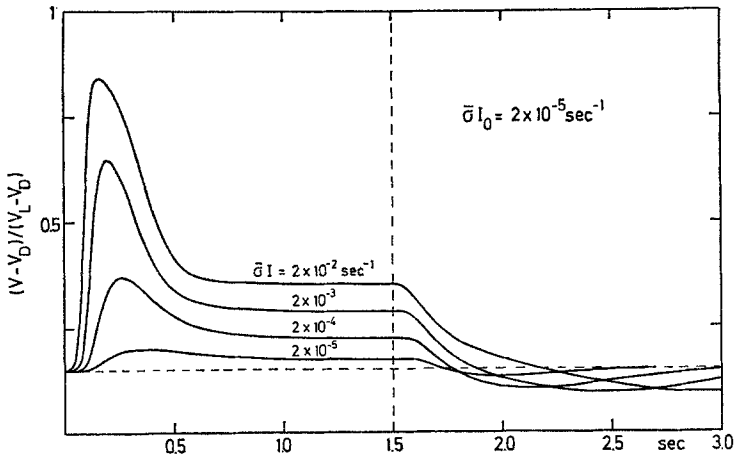

Fig. 11. Response to long stimulus superimposed on steady background light of intensity I_0. Same parameter as in Fig. 5

used. As a consequence of light adaptation (reduced A) the hight of the transient (even when measured from the dark potential) and the time delay of the response are reduced. At the plateau $V - V_D$ is of course equal to the plateau value for a single stimulus of intensity $I + I_0$. After turning off the test light there appears a transient hyperpolarization with respect to the potential maintained by the background light. This feature is yet another consequence of the delayed change of adaptation (which also produces the "normal" transient): When turning off the additional light, A is initially smaller than it would be in the steady state with just the background illumination turned on. Therefore at first x_A drops below its steady-state value until A has increased to its final value. Although we have not investigated this point, one expects oszillatory behavior in certain cases.

The features mentioned above are found in the *Limulus* lateral eye (Stieve *et al.*, 1975) although the interpretation is complicated by additional long-term adaptation processes which are probably due to changes in ionic gradients and active pump rates. The after-hyperpolarization in the presence of a background light has been known for some time (Stieve, 1965) and in Fig. 12 the intracellular recording from a *Limulus* lateral eye displaying this effect is shown.

Finally, let us point out that the changes which are found in the receptor potential after reduction of the calcium concentration in the extracellular solution can be simulated convincingly by the model. All one has to do is to reduce the rate of light adaptation. In Fig. 13a the effect of reducing p_2 from 600 sec^{-1} to 12 sec^{-1} and p_3 from 20 to 0.4 are shown for a short light flash. Whereas A is reduced in curve 1 to a minimum value of 0.89×10^{-2} at $t = 0.38$ sec, a minimum of 0.22 is reached in curve 2 at $t = 0.52$ sec. In Fig. 13b measurements on *Astacus* are shown. For a long light stimulus the reduction of p_2 and p_3 leads to a large increase of the height of the plateau in agreement with experiments (Stieve, 1965; Milecchia and Mauro, 1969a; Stieve and Wirth, 1971). For $p_2 = 0$ the transient disappears

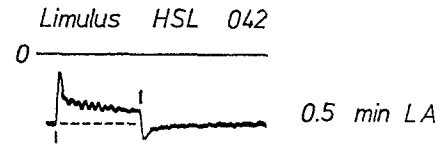

Fig. 12. Intracellular receptor potential following light stimulus of 2 sec duration and 30 sec after turning on a steady background light (Stieve *et al.*, 1975), $T \approx 22°$ C

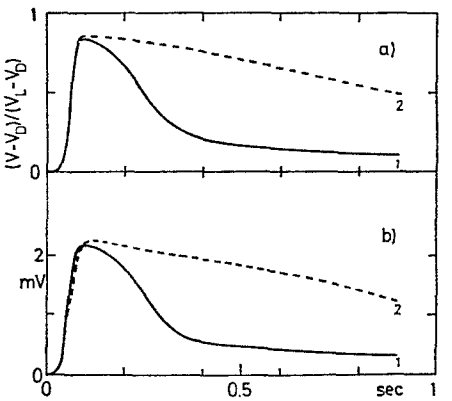

Fig. 13. a) Response to short light flash for $N = 10^5$, $k_0 = 130\ \text{sec}^{-1}$, $k_1 = 4\ \text{sec}^{-1}$, $k_2 = 40\ \text{sec}^{-1}$, $p_1 = 2\ \text{sec}^{-1}$, $p_2 = 600\ \text{sec}^{-1}$, $p_3 = 20$, $C = 40$, $V_L - V_D = 62.5$ mV (curve 1). In curve 2 p_2 was reduced to $12\ \text{sec}^{-1}$ and p_3 to 0.4. b) Response to short light flash in *Astacus* (Stieve and Wirth, 1971). Curve 2 was obtained after bathing retina for 60 min in Ca and Mg free solution. Curve 1 was obtained 60 min later after physiological conditions had been restored for 60 min

completely. It seems that for the reduction of the sensibility Ca has to be available (Weeks and Duncan 1974; Stieve and Hanani, 1975).

4. Discussion

Let us consider the initial phase of the receptor potential where the linear theory can be applied and saturation of the chain reactions can be disregarded [$Y(t, 0) \ll Z$]. After some multiplication has taken place [$Y(t, 0) \gg 1$] the response is found to depend on time and intensity in the following simple way

$$x_A \sim I \exp(k_0 t) = \exp[k_0 (t + k_0^{-1} \ln I)]. \tag{33}$$

Thus an increase in intensity simply shifts the initial phase of the response to earlier times, a phenomenon which can also be seen from Figs. 4, 5 and 9. This "shortening" of the latency period is a mere consequence of the linear superposition principle. The dependence of the shift on the logarithm of intensity is in fair agreement with experiments (Stieve *et al.*, 1975) although one seems to find a saturation at high intensities which is not contained in the model.

We have assumed the existence of one type of unit electrical responde to single photoisomerizations at low light intensity. This is probably a simplification of the true situation because at least two types of bumps are described in the literature (Borsellino and Fuortes, 1968a, b). Also, we have not considered the stochastic properties of the model. Since the chain reaction presumably consists of a large number of steps it can be treated deterministically. The stochastic variations of the single-photon response then consist primarily in variable time delays resulting from fluctuations in the reaction described by Eq. (22). In future work we hope to fit the rate constant k_1 to measurements of the latency distribution of receptor potential bumps.

Also, we plan to investigate the fluctuations of the model response in the nonlinear regime and compare it with experiments. It seems to us that the most critical tests for the type of activation kinetics proposed in Sect. 3 indeed comes from the study of the fluctuations rather than of the average response. It is hoped to proceed from here on towards an understanding of the actual mechanisms underlying activation and adaptation.

One of the most serious deficiencies of the model is in our opinion the unsatisfactory description of the electric membrane characteristics in the dark. The rough approximation made in Sect. 2 for the dark current bears consequences for the shape of the receptor potential which are difficult to estimate. Therefore, this point should be cleared up before other improvements of the model are considered. Alternatively, the influence of the dark current can be eliminated experimentally by using the voltage-clamp technique. When clamping the cell to the dark potential the current response is simply proportional to the degree of activation x_A. It would be very valuable to test under these conditions special features of the model, like the reduction of the single-photon contribution to the response with increasing activation, the shortening of the persistence time of the response with increasing x_A, and the appearance of a transient minimum in the activation after turning off a test light but maintaining a background illumination.

Finally, let us point out that by reinterpreting the process of activation in terms of a mechanism for blocking sites one can maybe apply the type of model proposed here to vertebrate photoreceptors.

Acknowledgement. This work was performed in close collaboration with the Institut für Neurobiologie, Kernforschungsanlage Jülich, Germany. The author is very grateful to Professor Dr. H. Stieve for suggesting this research, for numerous discussions and contributions during the course of the work and for critical reading of an earlier version of the manuscript. The author also wishes to thank Miss M. Bruns, Mrs. H. Gaube. Dr. T. Malinowska, Mr. K. Hartung and Dr. C. Krischer for valuable discussions and advice.

References

Allyn, M. R., Budrikis, Z. L.: A quantitative model of the response of the squid photoreceptor. To be published (1974)

Baylor, D. A., Hodgkin, A. L., Lamb, T. D.: Reconstruction of the electrical response of turtle cones to flashes and steps of light. J. Physiol. (Lond.) **242**, 759—791 (1974)

Borsellino, A., Fuortes, M. G. F., Smith, T. G.: Visual responses in *Limulus*. Cold Spr. Harb. Symp. quant. Biol. **30**, 429—443 (1965)

Borsellino, A., Fuortes, M. G. F.: Responses to single photons in visual cells of *Limulus*. J. Physiol. (Lond.) **196**, 507—539 (1968a)

Borsellino, A., Fuortes, M. G. F.: Interpretation of responses of visual cells of *Limulus*. Proc. I.E.E.E. **56**, 1024—1032 (1968b)

Cone, R. A.: The internal transmitter model for visual excitation: Some quantitative implications. In: Biochemistry and physiology of visual pigments (ed. H. Langer), pp. 275—281. Berlin-Heidelberg-New York: Springer 1973

Coster, H. G. L.: A quantitative analysis of the voltage-current relationships of fixed charge membranes and the associated property of "Punch-Trough". Biophys. J. **5**, 669—686 (1965)

Fuortes, M. G. F., Hodgkin, A. L.: Change in time scale and sensitivity in the ommatidia of *Limulus*. J. Physiol. (Lond.) **172**, 239—263 (1964)

Fuortes, M. G. F., O'Bryan, P. M.: Generator potentials in invertebrate photoreceptors. In: Handbook of sensory physiology, vol. VII/2 (ed. M. G. F. Fuortes), pp. 279—319. Berlin-Heidelberg-New York: Springer 1972

Krischer, G.: Photoreception of the barnacle, *Balanus eburneus*. Verh.Ber. d. Deutschen Zool. Ges., 64. Tagung, S. 165–169. Stuttgart: Fischer 1970

Levinson, J.: One-stage model for temporal integration. J. opt. Soc. Amer. **56**, 95–97 (1966)

Lisman, J. E., Brown, J. E.: Two light-induced processes in the photoreceptor cells of *Limulus* ventral eye. J. gen. Physiol. **58**, 544–561 (1971)

Mack Brown, H., Hagiwara, S., Koike, H., Meech, R. W.: Membrane properties of a barnacle photoreceptor examined by the voltage clamp technique. J. Physiol. (Lond.) **208**, 385–413 (1970)

Mack Brown, H., Hagiwara, S., Koike, H., Meech, R. W.: Electrical characteristics of a barnacle photoreceptor. Fed. Proc. **30**, 69–78 (1971)

Milecchia, R., Mauro, A.: The ventral photoreceptor cells of *Limulus* II. The basic photoresponse. J. gen. Physiol. **54**, 310–329 (1969a)

Milecchia, R., Mauro, A.: The ventral photoreceptor cells of *Limulus* III. A voltage-clamp study. J. gen. Physiol. **54**, 331–351 (1969b)

Stieve, H.: Interpretation of the generator potential in terms of inoic processes. Cold Spr. Harb. Symp. quant. Biol. **30**, 451–456 (1965)

Stieve, H., Wirth, C.: Über die Ionen-Abhängigkeit des Rezeptorpotentials der Retina von *Astacus leptodactylus*. Z. Naturforsch. **26b**, 457–470 (1971)

Stieve, H.: Mechanismen der Erregung von Lichtsinneszellen. Naturw. Rundschau **2**, 45–56 (1974a)

Stieve, H.: Unpublished (1974b)

Stieve, H.: Private communication (1975)

Stieve, H., Gaube, H., Winterhager, J.: On the effect of long-term light and dark adaptation and stimulus intensity on membrane characteristics of the *Limulus* photoreceptor cell, Ber. d. KFA Jülich, 1176 (1975)

Stieve, H., Hanani, M.: In preparation (1975)

Teorell, T.: Transport processes and electrical phenomena in ionic membrane. Progr. Biophys. **3**, 305–369 (1953)

Weeks, F. I., Duncan, G.: Photoreception by a Cephalopod Retina: Response Dynamics. Exp. Eye Res. **19**, 493–509 (1974)

Dr. Lorenz Kramer
Physik-Department
Technische Universität München
Theoretische Physik
D-8046 Garching b. München
James-Franck-Straße
Federal Republic of Germany